Normal contact stiffness of elastic solids with fractal rough surfaces for one- and three-dimensional systems

Roman Pohrt,[1] Valentin L. Popov,[1] and Alexander E. Filippov[2]
[1]*Berlin University of Technology, 10623 Berlin, Germany*
[2]*Donetsk Institute for Physics and Engineering of NASU, 83114 Donetsk, Ukraine*
(Received 12 March 2012; revised manuscript received 21 June 2012; published 20 August 2012)

It was shown earlier that some classes of three-dimensional contact problems can be mapped onto one-dimensional systems without loss of essential macroscopic information, thus allowing for immense acceleration of numerical simulations. The validity of this *method of reduction of dimensionality* has been strictly proven for contact of any axisymmetric bodies, both with and without adhesion. In [T. Geike and V. L. Popov, Phys. Rev. E **76**, 036710 (2007)], it was shown that this method is valid "with empirical accuracy" for the simulation of contacts between randomly rough surfaces. In the present paper, we compare exact calculations of contact stiffness between elastic bodies with fractal rough surfaces (carried out by means of the boundary element method) with results of the corresponding one-dimensional model. Both calculations independently predict the contact stiffness as a function of the applied normal force to be a power law, with the exponent varying from 0.50 to 0.85, depending on the fractal dimension. The results strongly support the application of the method of reduction of dimensionality to a general class of randomly rough surfaces. The mapping onto a one-dimensional system drastically decreases the computation time.

DOI: 10.1103/PhysRevE.86.026710 PACS number(s): 46.55.+d, 73.40.Cg, 62.20.Qp

I. INTRODUCTION

The roughness of surfaces has a great influence on many physical phenomena, such as friction, wear, sealing, adhesion, as well as electrical and thermal conductivity [1]. At the same time, it is one of the main reasons preventing the broad usage of numerical simulation methods in tribology—in contrast to many other contemporary areas in physics and engineering. Bowden and Tabor [2] were the first to realize the importance of the surface roughness of bodies in contact. Because of the roughness, the real contact area between the two bodies is typically orders of magnitude smaller than the apparent contact area. The works of Bowden and Tabor triggered an entirely new line of theory for contact mechanics regarding rough surfaces in the 1950s and 1960s with basic contributions by Archard [3] and Greenwood and Williamson [4]. The main result of these examinations was that the contact area between rough elastic surfaces is approximately proportional to the normal force. At the same time, it was realized that in many tribological problems, roughness on different spatial scales plays an important role in determining contact properties, friction, and wear. This understanding led in recent years to extensive studies of contact properties of bodies with rough surfaces [5–8]. The main focus of these studies was put on the determination of the real contact area for self-affine surfaces with relevant fractal dimensions. It was found that the contact area A is proportional to the normal force F_N and inversely proportional to the rms slope of the surface ∇h:

$A = \kappa F_N/(E^*\nabla h)$, where κ is near 2 and $E^* = [(1-\nu_1^2)/E_1 + (1-\nu_2^2)/E_2]^{-1}$ denotes the effective elastic modulus. E_1, E_2, ν_1, and ν_2 are the Young's moduli and Poisson ratios of the contacting bodies. Another important contact quantity, which is, however, much less investigated, is the *contact length*

$$\widetilde{L} = \frac{1}{E^*}\frac{\partial F}{\partial d}. \tag{1}$$

Here, d is the relative approach of the bodies. Note that d is not to be confused with the mean gap width. The notation of "contact length" stems from the fact that in the case of nonfractal rough surfaces, which can be described by the Greenwood and Williamson model (see [1] for details), this quantity really can be interpreted as the sum of the diameters of all contact regions. It is the contact length which determines many practically important properties, such as the electrical and thermal conductivity. The quantities related to the contact length are all connected with each other by exact analytical relations. For example, the electrical contact conductance Λ is linearly proportional to the incremental stiffness $k = (\partial F/\partial d) = E^*(\rho_1 + \rho_2)\Lambda/2$ [9], where ρ_1 and ρ_2 are the resistivities of the contacting bodies. Thus, the investigation of either the incremental stiffness or conductivity would suffice for determining this whole class of properties. Note that the properties associated with contact length force us to reconsider the question of what is a "complete contact." Due to the interdependence of all contact patches, it can be found that the saturation stiffness value corresponding to an ideal contact in macroscopic systems is reached long before a full material contact is established [1]. In other words, a relatively small real contact area suffices for causing the stiffness to be comparable to the full-contact indenter, as long as contact spots are equally spread over the apparent contact zone. The complete contact in the sense of electrical conductivity or stiffness is, therefore, reached much earlier than the complete "material contact."

In the present study, we concentrate our attention on the investigation of contact stiffness as the most physically relevant contact property. We do this both with the aid of the direct three-dimensional solution of the contact problem and by generating an "equivalent one-dimensional system" according to the prescriptions of the *method of reduction of dimensionality*. The main ideas of the method of reduction of dimensionality have been proposed in [10]. It has been

shown that there is a wide class of contacts between three-dimensional bodies, which can be mapped either exactly, or without loss of essential information, to one-dimensional systems (one-dimensional elastic or viscoelastic foundations). In 2007, Geike and Popov extended the basic ideas of this method to contacts of randomly rough surfaces [11,12]. In 2011, Heß proved many of the mapping theorems and showed that *exact* mapping is always possible for *any* axisymmetric body, both with and without adhesion [13]. The equivalence of three-dimensional systems to those of one dimension is valid for relations of the indentation depth, the contact area, and the contact force. The method of reduction of dimensionality has been applied later for the simulation of frictional forces in contacts of rough surfaces with elastomers [14–16]. A tangential contact problem with and without creep can also be mapped *exactly* to a one-dimensional system. It can further be shown that the reduction method is applicable to contacts of linear viscoelastic bodies as well as to thermal effects in contacts [17].

In this paper, an additional—and crucial—proof of the method of reduction of dimensionality is delivered through comparison of the contact stiffness between elastic solids with fractal surfaces (with fractal dimensions between 2 and 3) and the corresponding results from one-dimensional calculations with the method of reduction of dimensionality. These results also strongly support the applicability of the method of reduction of dimensionality to a wide spectrum of contact geometries and physical properties. The general structure of the paper is the following: In Sec. II, we present and discuss results of simulations of contact stiffness for true three-dimensional contacts of rough bodies. In Sec. III, we conduct the same calculations in the frame of the method of reduction of dimensionality. Section IV is finally devoted to the comparison of results and discussion of the physical nature of dependencies obtained.

II. CONTACT STIFFNESS OF THREE-DIMENSIONAL CONTACTS BETWEEN BODIES WITH FRACTAL ROUGH SURFACES

Recently, the contact stiffness was studied numerically, with the help of molecular dynamics [18] as well as with the boundary element method, and analytically, in the frame of Persson's contact theory [19,20]. According to the theory of Greenwood and Williamson [4], the contact stiffness k is approximately proportional to the normal force $k \approx \xi F/h$, where h is the rms roughness and ξ is a constant of the order of unity. In the theory of Persson, this proportionality must be exact [19]. Initially, numerical simulations carried out in [18] and [19], as well as experiments presented in [20], seemed to support this conclusion. However, recent simulations of the contact stiffness of bodies with fractal surfaces suggest that the dependence of the contact stiffness on the normal force can be reproduced much better by a power-law dependence, $k \propto F^{\alpha}$, with α ranging from 0.50 to 0.85, corresponding to a variation of fractal dimension from 2 to 3 [21].

This discrepancy partially stems from the difference between the two problems investigated in the literature: In [18–20] it is assumed that the fractal behavior is valid up to a specific, longest wavelength, the so-called "cutoff." Roughness having a longer wavelength is assumed to have an amplitude of zero. As the cutoff is much shorter than the actual system, simulations cannot map the whole indenter, if one wishes to take into account small wavelengths. Therefore, only a small patch from the inside of the indenter is simulated. Periodic boundary conditions are applied for taking into account the average of the surrounding patches that were not simulated. In this situation the stiffness is defined as the derivative of the normal force with respect to the mean gap width, as one cannot observe the indenter as a whole. In contrast to this, the Letter by Pohrt and Popov [21] assumes that the fractal behavior is valid all the way up to the system length itself. It is known that the contact stiffness is determined first of all by the long wavelength part of the power spectrum of the surface. However, as we are here considering fractal surfaces without cutoff, there is no scale separation between the "form" of the body as a whole and its "roughness" [22]. The interfacial separation cannot be defined unambiguously in this case. The relative approach of bodies is the only spatial variable which can be unambiguously defined for any finite contact. Therefore, in the case of fractal surfaces without cutoff, we use the approach instead of the interfacial separation. Furthermore, the use of the approach of the two bodies in the definition of the normal stiffness assures that results can be compared directly to experiments and that the proportionality to the electric conductivity as well as heat conductivity is given. In this scenario of course, boundaries are free, as they correspond to the physical edges of the indenter.

It is the author's strong belief that the proportionality found by Persson appears only in the first case described. Whenever the surfaces are truly fractal with no cut-off wavelength, a power law applies. In the present paper, we reproduce the results contained in the Letter by Pohrt and Popov [21] on the normal stiffness in more detail and complete them with calculations of an equivalent one-dimensional system. The extremely high spatial resolution used in this approach will exclude all doubts of size effects in the simulations. Furthermore, analytical considerations substantiate the power-law behavior in the region of small to medium normal forces.

We considered the normal contact between an elastic solid having a randomly rough self-affine surface with a flat, rigid body. The surface topography of the elastic body was characterized by its Fourier spectral density $C_{2D}(q)$,

$$C_{2D}(\vec{q}) = \frac{1}{(2\pi)^2} \int \langle f(\vec{x}) f(0) \rangle \exp(i\vec{x}\vec{q}) d\vec{x}. \tag{2}$$

For self-affine fractal surfaces, the spectral density has a power-law dependency on the wave vector

$$C_{2D}(q) = \text{const} \times \left(\frac{q}{q_0} \right)^{-2(H+1)}, \tag{3}$$

where H is the Hurst exponent, ranging from 0 to 1 [6]. This constant is directly related to the fractal dimension of a surface $D_f = 3 - H$. The surface topography is calculated in the two-dimensional case with the help of the power spectrum according to

$$h(\vec{x}) = \int_{q_{\min}}^{q_{\max}} dq\, B_{2D}(\vec{q}) \cos[\vec{q}\vec{x} + \varphi(\vec{q})], \tag{4}$$

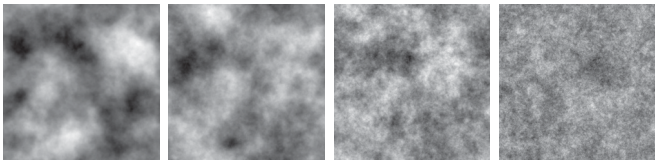

FIG. 1. Graphical representation of fractal surfaces having different fractal dimensions. Darker colors denote higher peaks in topography. Data has been scaled for giving optimal contrast in each picture.

where the phase $\varphi(\vec{q}) = \varphi(-\vec{q})$ is randomly distributed on the interval $[0,2\pi)$.

$\langle\varphi(\vec{q})\varphi(\vec{q}')\rangle = 2\pi\delta(\vec{q}-\vec{q}')$ and density $B_{2D}(\vec{q}) = B_{2D}(-\vec{q})$ is determined by the spectral density $C_{2D}(\vec{q})$ using the relation

$$B_{2D}(\vec{q}) = \frac{2\pi}{L}\sqrt{C_{2D}(\vec{q})}. \tag{5}$$

The integration in Fourier space is limited by two characteristic wave vectors $q_{\min}$ and $q_{\max}$ to which the scale-invariant behavior is restricted. In the present work, these limits were chosen as the longest and shortest wavelengths that could be represented on the chosen grid size. Figure 1 shows a graphical representation of typical surface shapes for different values of D_f in a gray-scale map, where darker colors denote higher peaks in topography. Rough surfaces were generated on a square A_0 with an equidistant discretization of 2049×2049 points. The slightly bizarre-looking surface shape is due to the aforementioned fact that in the present paper we consider surfaces without large cut-off wavelength. For low fractal dimensions, this effect is directly visible, because the longest wavelength dominates and creates an apparently wide, global maximum.

We applied the boundary element method with an iterative multilevel algorithm to obtain the pressure distribution for a series of dimensionless normal forces ranging from 10^{-8} to 20 [see Eq. (10) for definition]. The incremental stiffness k was calculated by evaluating the differential quotient of force and indentation depth. All values were obtained by an ensemble averaging over 60 surface realizations having the same power spectrum. As the stiffness at complete contact is saturated at $k_s = 1.012 \times 2E^*\sqrt{A_0/\pi} = 1.1419 \times E^*\sqrt{A_0}$ [1], it is sensible to define a dimensionless stiffness as $\bar{k}_i = k(d_i)/(1.1419 \times E^*\sqrt{A_0})$. The computation grid naturally imposes a lower boundary for the numerical stiffness in the case where a single discrete grid point is in contact. Stiffness values near that boundary are, therefore, omitted. The calculated dependencies of the contact stiffness on the normal force for six fractal dimensions ($D_f = 2.0,2.2,2.4,2.6,2.8,3.0$) are shown in Fig. 2. For low to medium forces, the logarithm of stiffness is very accurately proportional to the logarithm of the normal force, the stiffness being a power function of force $\bar{k} = \text{const} \times \bar{F}^{\alpha}$. The power α can be fitted as

$$\alpha \approx 0.266 D_f, \tag{6}$$

(see Fig. 3). This result qualitatively differs from the prediction $\bar{k} \approx \xi F/h$ of the Greenwood and Williamson model, but corresponds much better to the experimental measurements of contact stiffness reported in [23].

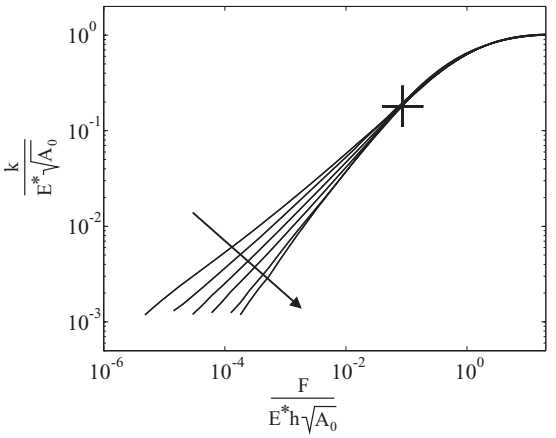

FIG. 2. Dimensionless incremental stiffness on the dimensionless normal force. Dependencies are shown for $D_f = 2.0,2.2,2.4,2.6,2.8,3.0$, as indicated by the arrow.

Based on the power law, we searched for an analytical approximation for the contact stiffness. Under the assumption that the only parameters appearing in the stiffness-force dependence are the elastic modulus E^* and the rms roughness h and that it is a power-law function of all arguments, the problem contains only the following independent dimensionless variables:

$$\text{dimensionless stiffness } \bar{k} = \frac{k}{1.1419 \times E^*\sqrt{A_0}},$$
$$\text{dimensionless force } F/(E^*A_0),$$
$$\text{and dimensionless roughness } h/\sqrt{A_0}.$$

The general form of a power function connecting these variables is

$$\frac{k}{1.1419 \times E^*\sqrt{A_0}} = \zeta\left(\frac{F}{E^*A_0}\right)^{\alpha}\left(\frac{h^2}{A_0}\right)^{\delta}, \tag{7}$$

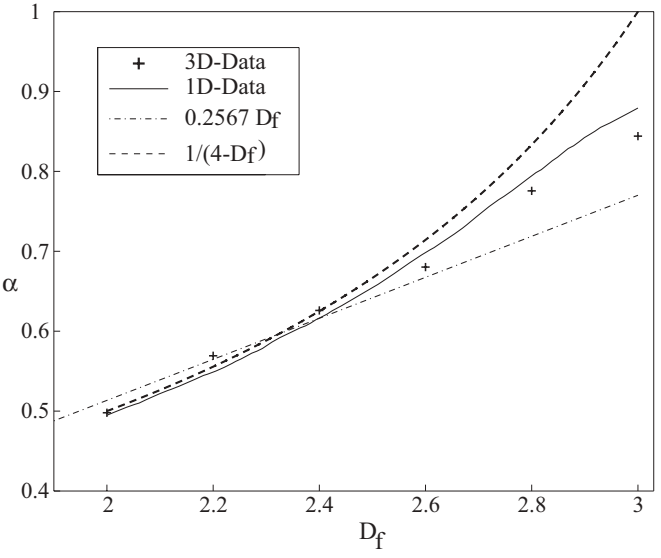

FIG. 3. Dependence of power α in (8) on the fractal dimension of a surface. Results from 3D Boundary Element Method and 1D reduction method are shown. The curved dashed line represents the analytical result (24).

where ζ is a dimensionless constant. This dependence must possess the following strict scaling properties. If the vertical scale of the surface inhomogeneity is multiplied by a certain factor, then the contact configuration does not change, provided that the force F and the indentation depth u_z are both multiplied by the same factor. This means that k does not change and the relation $\alpha + 2\delta = 0$ is valid; it follows that $\delta = -\alpha/2$. In addition, at a given contact configuration, both the force and the stiffness must be strictly proportional to the effective elastic modulus E^*, which is already fulfilled by the above equation. The only possible general power dependence of the contact stiffness on force obeying these scaling relations is

$$\frac{k}{1.1419 \times E^*\sqrt{A_0}} = \zeta\left(\frac{F}{E^*h\sqrt{A_0}}\right)^{\alpha}, \tag{8}$$

$$\overline{k} = \zeta\,\overline{F}^{\alpha}, \tag{9}$$

with dimensionless force

$$\overline{F_N} = \frac{F}{E^*h\sqrt{A_0}}. \tag{10}$$

As can be seen from Fig. 2, all curves collapse for $\overline{k_{\rm ul}} = 0.18$ and $\overline{F_{\rm ul}} = 0.086$, giving the upper limit for which the power law is valid. This intersection also tells us how to correctly choose the coefficient ζ as a function of the fractal dimension:

$$\frac{\overline{k}}{\overline{k_{\rm ul}}} = \left(\frac{\overline{F}}{\overline{F_{\rm ul}}}\right)^{0.266D_f} \Rightarrow \zeta = \frac{\overline{k_{\rm ul}}}{\overline{F_{\rm ul}}^{0.266D_f}}. \tag{11}$$

Finally we find the following approximation for the stiffness:

$$\frac{k}{1.1419 \times E^*\sqrt{A_0}} = 0.18\left(\frac{F}{0.086E^*h\sqrt{A_0}}\right)^{0.266D_f}. \tag{12}$$

To prove this relation, the value of $\tilde{F} = \overline{F_{\rm ul}}[\bar{k}/\overline{k_{\rm ul}}]^{1/0.266D_f}$ is plotted versus the dimensionless normal force $\bar{F} = F/(E^*h\sqrt{A_0})$ in Fig. 4. The data for all forces and all fractal dimensions collapse to one master curve.

Using the exact relation between the constriction conductance Λ and the incremental stiffness of a contact between two bodies [9], we can straightforwardly write down an expression for the contact conductance of bodies having rough surfaces and resistivities ρ_1 and ρ_2:

$$\Lambda = \frac{0.411\sqrt{A_0}}{(\rho_1 + \rho_2)}\left(\frac{F}{0.086 \times E^*h\sqrt{A_0}}\right)^{0.266D_f}. \tag{13}$$

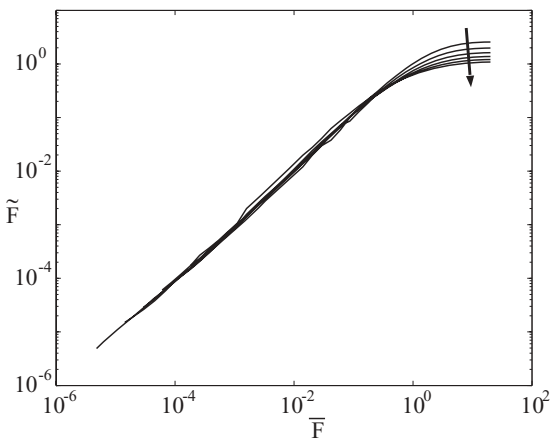

FIG. 4. A plot of $\tilde{F} = \overline{F_{\rm ul}}[\bar{k}/\overline{k_{\rm ul}}]^{1/0.266D_f}$ shows that the valid range for Eq. (12) comprises four orders of magnitude in dimensionless $\bar{F}$ with the chosen resolution of 2049 × 2049. Fractal dimensions are chosen as in Fig. 2.

III. CONTACT STIFFNESS OF AN EQUIVALENT ONE-DIMENSIONAL SYSTEM

We now solve the same problem with the method of reduction of dimensionality, first demonstrated for single contacts [10] and extended to rough surfaces with a constant spectral density [11,12]. The method was verified later in applications to surfaces with various fractal properties by a comparison of the results with the data for three-dimensional models existing in literature.

According to this method, the original three-dimensional body can be formally substituted by an equivalent one-dimensional "rough line"

$$h(\vec{x}) \to h(x) = \int_{q_{\rm min}}^{q_{\rm max}} dq\; B_{\rm 1D}(q)\cos[qx + \varphi(q)], \tag{14}$$

with Fourier coefficients defined by the one-dimensional spectral density $C_{\rm 1D}(q)$:

$$B_{\rm 1D}(q) = \sqrt{\frac{2\pi}{L}C_{\rm 1D}(q)}, \tag{15}$$

with an elastic foundation with normal stiffness per length equal to

$$k = E^*. \tag{16}$$

To be equivalent to the initial three-dimensional body, the one-dimensional spectral density $C_{\rm 1D}(q)$ has to be defined according to [1,11]

$$C_{\rm 1D}(q) = \pi q C_{\rm 2D}(|\vec{q}|). \tag{17}$$

This choice ensures that the one-dimensional rough line has the same rms roughness as well as the same moments and moments of derivatives of the surface profile as the three-dimensional original. In the case of self-affine rough surfaces, the three-dimensional (3D) and one-dimensional (1D) bodies will have the same Hurst exponent. Just as in the 3D case, the integration in Fourier space is limited by two characteristic cut-off wave vectors $q_{\rm min}$ and $q_{\rm max}$ to which the scale-invariant behavior is restricted.

Finally, to ensure that the contact properties at a complete contact are identical in the one- and three-dimensional cases, the length $L_{\rm 1D}$ of the one-dimensional system must be chosen to be equal to the diameter of the three-dimensional system [or in the case of a square indenter with the area A_0, the equivalent one-dimensional length is determined by the condition $(\pi/4)L_{\rm 1D}^2 = A_0$], thus,

$$L_{\rm 1D} = \frac{2}{\sqrt{\pi}}A_0^{1/2}. \tag{18}$$

Typical curves $h(x)$ calculated for $2^{20} \approx 10^6$ elements for two limiting fractal dimensions $D_f = 3, D_f = 2$ and one intermediate dimension $D_f = 2.5$ are shown, respectively, in

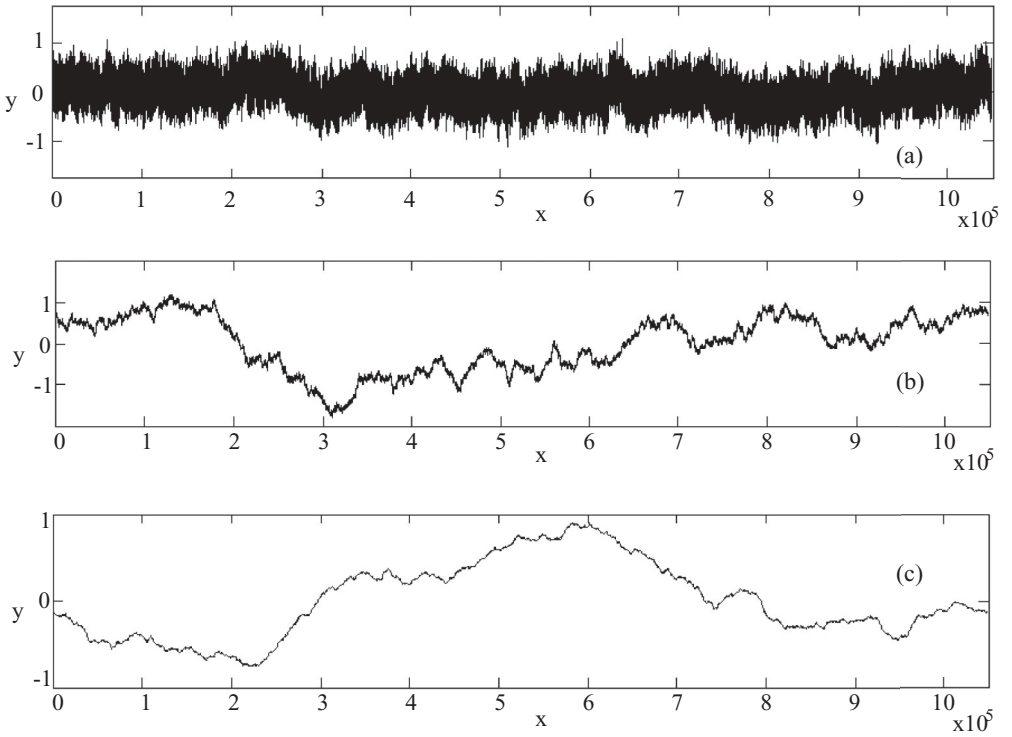

FIG. 5. One-dimensional realizations corresponding to fractal surfaces with different fractal dimensions D_f. Subplots (a), (b), and (c) correspond, respectively, to $D_f = 3, D_f = 2.5$, and $D_f = 2$.

the suplots (a), (b), and (c) of Fig. 5. Fractal dimensions always refer to the three-dimensional original and not to the one-dimensional system.

One can see that the change of the fractal dimension D_f leads to a transformation of the steady, but highly noise-afflicted line for large fractal dimensions to an essentially "nonplanar" curve for small fractal dimensions. This nonplanarity is a universal feature for "true fractal" surfaces, for which $q_{\min}$ is determined by the size L of the system. To obtain statistically reliable data, we performed an ensemble averaging of all of the results over 500 surface realizations having the same power spectrum. A different number of realizations compared to 3D simulations is only due to the "low computation cost" of 1D results.

The results are presented in Fig. 6. As in the three-dimensional case, the dependencies of the contact stiffness on normal force are power-law functions at small force and transition to a plateau at large normal forces. The values of the stiffness at the plateau are exactly the same in the 1D and 3D cases [the length of the one-dimensional system (18) was chosen so that they are exactly equal]. The saturation value of the stiffness is reached in both cases for forces of about $F = 20(E^* h\sqrt{A_0})$. The parameters of the dependencies of stiffness on the normal force for the 1D case have been plotted in Figs. 3 and 7 together with results for the 3D case. It is seen that the 1D and 3D results agree very well. In the region of practically relevant fractal dimensions between 2 and 2.5, they coincide almost exactly. Note that in the 1D case, we investigated an even wider range of forces than in the 3D case. In the 1D case, the power-law dependencies remain correct up to forces of 10^{-7} if the surface is still fractal at very small wavelengths. In the 3D case, we simply had no technical possibility to prove this: Grid sizes in 3D that would allow for these small contact areas to be reproduced correctly cannot be calculated within a reasonable time, not even with the multigrid techniques we have been using.

The overall scaling coefficient ζ as shown in Fig. 7, has the same order of magnitude in both cases, but does not coincide exactly. Therefore, a more thorough investigation of the vertical scaling of the system depending on the fractal dimension is needed. Note that for simple rotationally symmetric forms, a vertical rescaling of the system is needed as well [1,11,13]. The only region where there is a systematical discrepancy between 1D and 3D cases is the region of crossover from

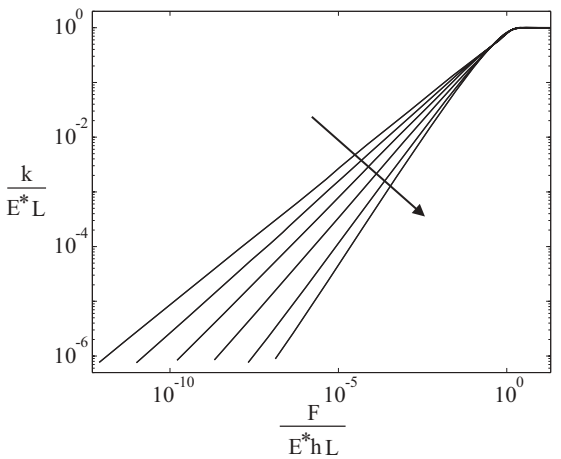

FIG. 6. Dependencies of the dimensionless incremental stiffness on the dimensionless normal force shown in logarithmic coordinates. Results have been obtained with the 1D reduction method.

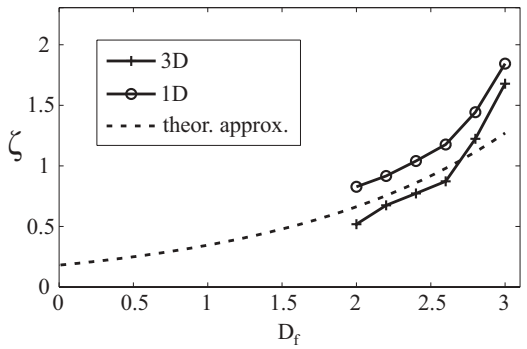

FIG. 7. Dependence of the coefficient ζ on the fractal dimension can be approximated as $\zeta \approx \overline{k_{\mathrm{ul}}}/\overline{F_{\mathrm{ul}}}^{0.266D_f}$.

the power-law dependency to the plateau. In the 1D case, the stiffness is overestimated by up to 25% in this region and the saturation is reached more quickly.

IV. COMPARISON OF ONE-DIMENSIONAL AND THREE-DIMENSIONAL SIMULATIONS AND DISCUSSION

Comparison of three-dimensional and one-dimensional results shows that they agree well both qualitatively and quantitatively over many orders of magnitude of normal forces and for all fractal dimensions between 2 and 3. While the validity of the method of reduction of dimensionality has been proven earlier exactly for any bodies of revolution [13] and with engineering accuracy of several percent for dependencies of contact area on the normal force, the results of the present paper support its validity for a further, and very important, class of properties related to the contact length for fractal dimensions between 2 and 3 and for forces changing over at least four decimal orders of magnitude. The crossover to the constant stiffness at the "complete contact" is also qualitatively correct and the limiting value of the contact stiffness at the plateau is the same in one-dimensional and three-dimensional cases. The huge difference between the three-dimensional and one-dimensional calculations is, however, in the computation time: While the entire set of three-dimensional calculations presented in Fig. 2 require several weeks, the corresponding one-dimensional results were obtained in a few seconds.

There are analytical considerations supporting the power-law dependence of the contact stiffness and the strict equivalence of three-dimensional and one-dimensional results for small fractal dimensions. As can easily be seen from Fig. 1 or Fig. 5, in this case the surface has a pronounced nonplanarity on the largest scale. Therefore, the contact at small contact force is localized in the vicinity of the global maximum within the apparent contact area. On the largest scale, there is only one contact region visible, although it may be subdivided into smaller sections when magnified. Now, let us zoom closer into that one contact region to get an indentation of the magnified surface with the new length L':

$$\begin{aligned} L' &= CL \quad \text{or} \quad A' = C^2 A, \\ d' &= d. \end{aligned} \tag{19}$$

According to the definition of a self-affine surface, this transformation provides a surface with the same statistical properties, so

$$h' = C^H h. \tag{20}$$

The transformation (19) lets the complete "contact state," including the contact force and contact stiffness remain unchanged:

$$\begin{aligned} F' &= F, \\ k' &= k. \end{aligned} \tag{21}$$

In terms of the dimensionless variables motivated above, we get

$$\begin{aligned} C\overline{k'} &= \bar{k}, \\ C^{H+1}\overline{F'} &= \bar{F}. \end{aligned} \tag{22}$$

Eliminating the arbitrary scaling C leads to

$$(\bar{F}/\overline{F'})^{1/(H+1)} = (\bar{k}/\overline{k'}), \tag{23}$$

confirming not only the power law itself but also directly supplying a value for the exponent:

$$\alpha = \frac{1}{1+H}. \tag{24}$$

In Fig. 3, for comparison, the function (24) is plotted together with empirical dependencies obtained from numerical simulations. Note that the equivalent one-dimensional system produced with spectral density calculated according to the rule (17) has the same Hurst exponent. The one-dimensional analog of Eq. (8) reads

$$\frac{k}{E^* L} \propto \left(\frac{F}{E^* h L}\right)^{\alpha}. \tag{25}$$

The above scaling considerations are applicable to the one-dimensional case without any changes and lead to the same result (24) for the exponent α. Thus, both the power dependence of contact stiffness for self-affine fractal rough surfaces and the equivalence of three-dimensional results to those produced for one dimension according to the rules of the method of reduction of dimensionality are exact.

In conclusion, the boundary element method and the reduction method were used to study the normal stiffness of elastic bodies with self-affine randomly rough surfaces with fractal dimensions ranging from 2 to 3. The linear dependence of the contact area on the normal force predicted by Persson's theory was found, but we obtained a nonlinear behavior for the incremental normal stiffness. It appears to be a power-law dependence of the normal force with the power ranging from 0.50, for a fractal dimension of $D_f = 2$, to 0.85, for a fractal dimension of $D_f = 3$. We have found simple analytical approximations for contact stiffness and contact conductance, which are valid over more than three orders of magnitude of normal force.

ACKNOWLEDGMENTS

The authors are grateful to R. Wetter for attracting attention to the paper by J. R. Barber. This material is based upon work supported by AiF (Grant No. KF2293701WZ9) and by the Deutsche Forschungsgemeinschaft (DFG, Grant No. PO 810/24-1).

[1] V. L. Popov, *Contact Mechanics and Friction* (Springer, Berlin, 2010).
[2] F. P. Bowden and D. Tabor, *The Friction and Lubrication of Solids* (Clarendon Press, Oxford, 1986).
[3] J. F. Archard, Proc. R. Soc. London, Ser. A **243**, 190 (1957).
[4] J. A. Greenwood and J. B. P. Williamson, Proc. R. Soc. London, Ser. A **295**, 300 (1966).
[5] S. Hyun, L. Pei, J.-F. Molinari, and M. O. Robbins, Phys. Rev. E **70**, 026117 (2004).
[6] B. N. J. Person, Surf. Sci. Rep. **61**, 201 (2006).
[7] S. Hyun and M. O. Robbins, Tribol. Int. **40**, 1413 (2007).
[8] C. Campana and M. H. Müser, Phys. Rev. B **74**, 075420 (2006).
[9] J. R. Barber, Proc. R. Soc. Lond. A **459**, 53 (2003).
[10] V. L. Popov and S. G. Psakhie, Tribol. Int. **40**, 916 (2007).
[11] T. Geike and V. L. Popov, Phys. Rev. E **76**, 036710 (2007).
[12] T. Geike and V. L. Popov, Tribol. Int. **40**, 924 (2007).
[13] M. Heß, *Über die Abbildung ausgewählter dreidimensionaler Kontakte auf Systeme mit niedrigerer räumlicher Dimension* (Cuvillier-Verlag, Göttingen, 2011).
[14] V. L. Popov and A. E. Filippov, Tech. Phys. Lett. **36**, 525 (2010).
[15] V. L. Popov and A. V. Dimaki, Tech. Phys. Lett. **37**, 8 (2011).
[16] A. E. Filippov and V. L. Popov, Phys. Rev. E **75**, 027103 (2007).
[17] V. L. Popov, *Kontaktmechanik und Reibung*, 2nd ed. (revised) (Springer, Berlin, Heidelberg, 2009).
[18] S. Akarapu, T. Sharp, and M. O. Robbins, Phys. Rev. Lett. **106**, 204301 (2011).
[19] C. Campana, B. N. J. Persson, and M. H. Müser, J. Phys.: Condens. Matter **23**, 085001 (2011).
[20] B. Lorenz and B. N. J. Persson, J. Phys.: Condens. Matter **21**, 015003 (2009).
[21] R. Pohrt and V. L. Popov, Phys. Rev. Lett. **108**, 104301 (2012).
[22] V. L. Popov, J. Starcevic, and A. E. Filippov, Phys. Rev. E **75**, 066104 (2007).
[23] R. Buzio, C. Boragno, F. Biscarini, F. B. de Mongeot, and U. Valbusa, Nat. Mater. **2**, 233 (2003).